

Numerical investigation of circular and square tubes subjected to low velocity impact load

Hung Anh LY*, Thinh THAI-QUANG

Department of Aerospace Engineering, Faculty of Transportation Engineering, Ho Chi Minh City University of Technology, Ho Chi Minh City, Vietnam

Email address:

lyhunganh@hcmut.edu.vn (H. A. LY), quang_thinh1207@yahoo.com (T. THAI-QUANG)

To cite this article:

Hung Anh LY, Thinh THAI-QUANG. Numerical Investigation of Circular and Square Tubes Subjected to Low Velocity Impact Load.

International Journal of Mechanical Engineering and Applications. Special Issue: Transportation Engineering Technology.

Vol. 3, No. 1-3, 2015, pp. 54-62. doi: 10.11648/j.ijmea.s.2015030103.19

Abstract: Crash-dynamics research has contributed significantly to the safety, survivability of passengers in transportation accidents, especially in automotive industry. Among thin-walled structures, the application of thin-walled tubes with square and circular cross-sections has gained currency thanks to convenience of manufacture and capability of energy absorption. To identify these characteristics, it has been a wide range of studies in theoretical, numerical and experimental analysis. Throughout the progression and proliferation, moreover, there have been many improvements, corrections in both theories and numerical simulations. However, it is lack of a systematic results and comprehensive remarks. Hence, in this paper, a thorough review will be illustrated and comments, specific guidance will be introduced in theoretical calculation and numerical simulation as well.

Keywords: Crash-dynamics, Thin-walled structures, Square tubes, Circular tubes

1. Literature review

1.1. Circular Tube

Alexander's model for axisymmetric static crushing mode

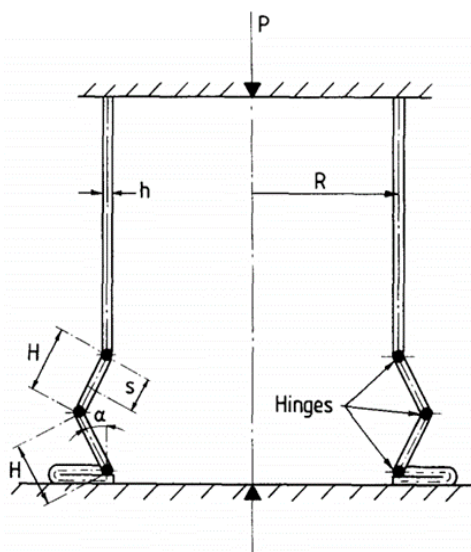


Figure 1. Assumed collapse mode [2].

To address the energy absorption of thin cylindrical shells under axial loading, in 1960, Alexander [1] firstly proposed an approximate solution for axisymmetric static crushing mode. In his analysis, for simplified purposes, Alexander assumed that elastic strains and work hardening of the material are ignored, i.e. a “plastic-rigid” material and used the simplified axisymmetric deformation pattern with plastic hinges which is illustrated in Fig. 1. This is also an ideal case of practical behavior due to the fact that the profile of the wrinkles are curved instead of straight as shown in Fig. 2. However, this method also has some meanings for design purposes because it gave some initial results which has been used in numerical and experimental analyses afterwards. In addition, Alexander's solution inspired other researchers to develop and improve this model in a better way. Alexander concluded the axial crushing force P_m for axisymmetric static crushing mode is [2]

$$\frac{P_m}{M_0} = 20.73 \left(\frac{2R}{h} \right)^{1/2} + 6.283 \quad (1)$$

where R is the tube radius, h is the thickness of the tube and

$$M_0 = \left(\frac{2\sigma_0}{\sqrt{3}}\right) \left(\frac{h^2}{4}\right) \quad (2)$$

where σ_0 is uniaxial yield stress.

Additionally, length of a basic element $2H$ is [2]

$$\frac{H}{R} = 1.905 \left(\frac{h}{2R}\right)^{1/2} \quad (3)$$

Abramowicz et al.'s modification for axial crushing modes relied on Alexander's solution

In 1984, Abramowicz et al. [3] suggested a correction for mean static crushing force P_m and length of a basic element $2H$, respectively

$$\frac{P_m}{M_0} = 20.79 \left(\frac{2R}{h}\right)^{1/2} + 11.90 \quad (4)$$

$$\frac{H}{R} = 1.76 \left(\frac{h}{2R}\right)^{1/2} \quad (5)$$

for symmetric, or concertina mode.

To non-axisymmetric (diamond mode) crushing,

$$\frac{\bar{P}_m^d}{M_0} = \left(\frac{20.79(2R/h)^{1/2} + 11.90}{0.86 - 0.568(h/2R)^{1/2}}\right) \left[1 + \left(\frac{0.25V}{6844R(0.86 - 0.568(h/2R)^{1/2})}\right)^{1/3.91}\right] \quad (9)$$

and

$$\frac{\bar{P}_m^d}{M_0} = 86.14(2R/h)^{1/3} \left[1 + \left(\frac{0.37V}{6844R}\right)^{1/3.91}\right] \quad (10)$$

for symmetric and non-symmetric crushing mode, respectively.

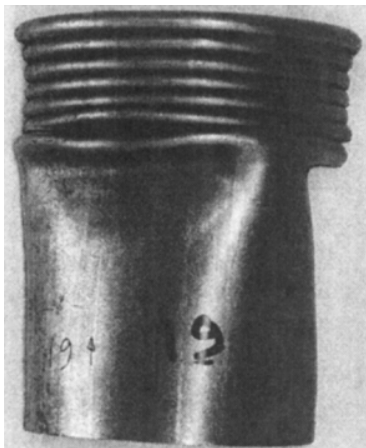


Figure 2. Static axial crushing of a thin-walled steel cylindrical shell [2].

Further improvement of Abramowicz et al. for axial crushing modes from Alexander's theory

The modification of Abramowicz et al. in 1986 [8] is the change of the energy dissipated in plastic hinges E_1 of [3] when the actual deformed profile of one lobe is idealized as in Fig. 3. The mean static crushing load is

Abramowicz summarized from [4] and gave an approximate expression for mean axial static crushing force and distance of a basic element which had good agreement with experimental results, respectively

$$\frac{P_m}{M_0} = 62.88 \left(\frac{2R}{h}\right)^{1/3} \quad (6)$$

$$\frac{H}{R} = 0.816 \left(\frac{h}{2R}\right)^{1/3} \quad (7)$$

When considering effective crushing distance, Abramowicz based on [5], results from [6]

$$\frac{\delta_e}{2H} = 0.73 \quad (8)$$

Regarding material strain rate effects, constitutive equation of Cowper-Symonds was employed with $D = 6844 \text{ s}^{-1}$ and $p = 3.91$ [6] agreed with a wide range of experimental data that Campell and Cooper [7] experimented the ultimate tensile stresses of the steel specimens. Finally, the mean dynamic loads of a circular tube is [3]

$$\frac{\bar{P}_m}{M_0} = \frac{25.23(2R/h)^{1/2} + 15.09}{0.86 - 0.568(h/2R)^{1/2}} \quad (11)$$

and the distance of a basic folding element is

$$H/R \cong 1.84(h/2R)^{1/2} \quad (12)$$

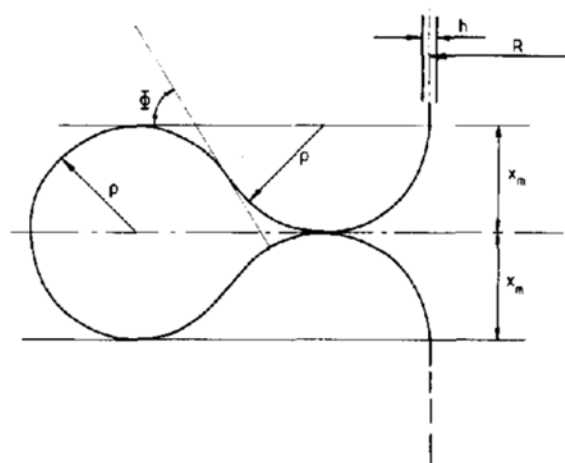


Figure 3. Deformed lobe [8].

In addition, Abramowicz et al. summarized a predicted expression for non-axisymmetric (diamond mode) crushing

$$\frac{\bar{P}_m}{M_0} = A_{3N}(2R/h)^{1/2} + A_{4N} \quad (13)$$

where $A_{3N} = 31.01, 28.86, 28.23, 27.95$ and 27.81 corresponding to $A_{4N} = 17.22, 44.74, 83.15, 132.49$ and

$$\frac{\bar{P}_m^d}{M_0} = \left(\frac{25.23(2R/h)^{1/2} + 15.09}{0.86 - 0.568(h/2R)^{1/2}} \right) \left[1 + \left(\frac{0.25V}{6844R(0.86 - 0.568(h/2R)^{1/2})} \right)^{1/3.91} \right] \quad (14)$$

for axisymmetric behavior, or concertina mode and

$$\frac{\bar{P}_m^d}{M_0} = (A_{3N}(2R/h)^{1/2} + A_{4N}) \left[1 + \left(\frac{A_{5N}V(h/2R)^{1/2}}{6844R} \right)^{1/3.91} \right] \quad (15)$$

for non-axisymmetric behavior, or diamond mode, where $A_{5N} = 0.171, 0.716, 1.814, 3.648$ and 6.404 corresponding to $N = 2, 3, 4, 5$ and 6 , respectively.

1.2. Square tube

Model of Abramowicz et al. [6]

To study the crushing process of thin-walled structures, in 1984, Abramowicz et al. based on [9] to make some assumptions, thereby identifying the two basic folding elements shown in Fig. 4 which has been used to predict the static axial progressive buckling of square tubes with a mean width c and a mean wall thickness h . This is also revised in [10].

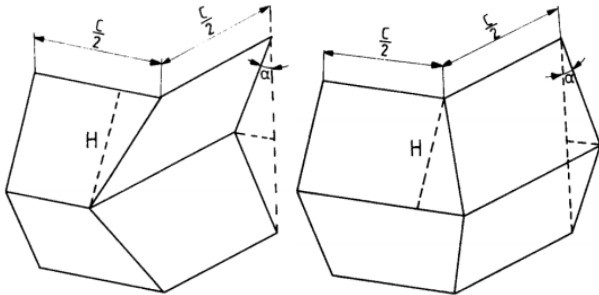


Figure 4. Basic collapse elements, Left: Type I; Right: Type II [6].

The idealized symmetric collapse mode shown in Fig. 5 comprises four type I elements. The mean static crushing force is predicted [6]

$$\frac{P_m}{M_0} = 38.12 \left(\frac{c}{h} \right)^{1/3} \quad (16)$$

with

$$\frac{H}{h} = 0.99 \left(\frac{c}{h} \right)^{2/3} \quad (17)$$

where

$$M_0 = \frac{\sigma_0 h^2}{4} \quad (18)$$

192.80 when the number of circumferential lobes (N) is 2, 3, 4, 5 and 6, respectively.

Examining material strain rate effects, the mean dynamic crushing force of a circular tube is respectively [8]

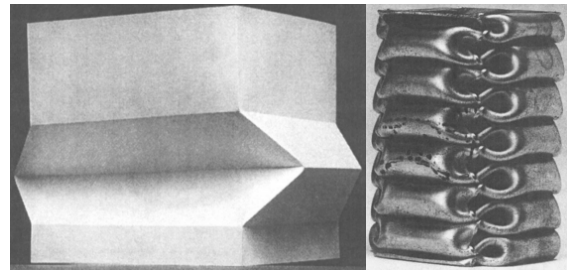


Figure 5. Symmetric collapse mode, Left: Paper model; Right: Actual specimen [2].

It can be inferred from Fig. 6 that the asymmetric mixed collapse mode A includes two layers with a total initial height $4H$ and six type I and two type II basic folding elements. The mean static crushing force is given by [6]

$$\frac{P_m}{M_0} = 33.58 \left(\frac{c}{h} \right)^{1/3} + 2.92 \left(\frac{c}{h} \right)^{2/3} + 2 \quad (19)$$

with

$$\frac{H}{h} = 0.73 \left(\frac{c}{h} \right)^{2/3} \quad (20)$$

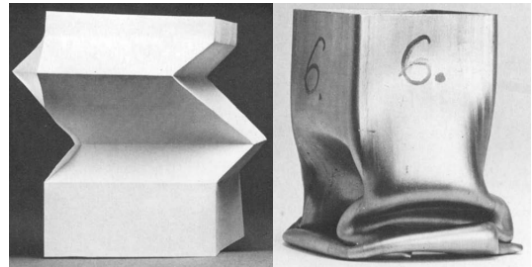


Figure 6. Asymmetric mixed collapse mode A, Left: Paper model; Right: Actual specimen [6].

Regarding to asymmetric mixed collapse mode B, it can be seen in Fig. 7, this mode consists of two layers with a total initial height $4H$ and seven type I and one type II basic folding elements. The mean static crushing force is given by [6]

$$\frac{P_m}{M_0} = 35.54 \left(\frac{c}{h}\right)^{1/3} + 1.65 \left(\frac{c}{h}\right)^{2/3} + 1 \quad (21)$$

with

$$\frac{H}{h} = 0.83 \left(\frac{c}{h}\right)^{2/3} \quad (22)$$

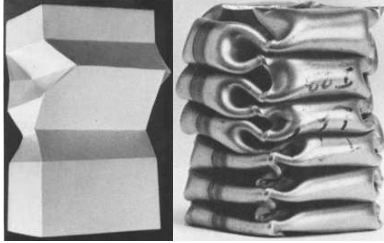


Figure 7. Asymmetric mixed collapse mode B, Left: Paper model; Right: Actual specimen [6].

From Fig. 8, extensional collapse mode includes one layer with four type II elements. The mean static crushing force [6]

$$\frac{P_m}{M_0} = 16\sqrt{\pi} \left(\frac{c}{h}\right)^{1/2} + 8 \quad (23)$$

with

$$\frac{H}{h} = 0.886 \left(\frac{c}{h}\right)^{1/2} \quad (24)$$

Examining effective crushing distance and material strain rate sensitivity, the mean dynamic crushing loads are



Figure 8. Extensional collapse mode [2].

$$\frac{\bar{P}_m^d}{M_0} = 52.22 \left[1 + \left(\frac{0.33V}{cD}\right)^{1/p} \right] \left(\frac{c}{h}\right)^{1/3} \quad (25)$$

$$\frac{\bar{P}_m^d}{M_0} = \left[1 + \left(\frac{0.49V}{cD}\right)^{1/p} \right] \left[43.61 \left(\frac{c}{h}\right)^{1/3} + 3.79 \left(\frac{c}{h}\right)^{2/3} + 2.6 \right] \quad (26)$$

$$\frac{\bar{P}_m^d}{M_0} = \left[1 + \left(\frac{0.41V}{cD}\right)^{1/p} \right] \left[46.16 \left(\frac{c}{h}\right)^{1/3} + 2.14 \left(\frac{c}{h}\right)^{2/3} + 1.3 \right] \quad (27)$$

for the symmetric mode, asymmetric mixed collapse mode A, asymmetric mixed collapse mode B, respectively.

Further improvements of Abramowicz et al. [8]

In 1986, Abramowicz et al. corrected by consideration of an improved kinematic mechanism (presented in the Appendix in [8]). With this correction, the mean static crushing force and length of a basic folding element are

$$\frac{P_m}{M_0} = 33.05 \left(\frac{c}{h}\right)^{1/3} + 2.44 \left(\frac{c}{h}\right)^{2/3} + \frac{\pi}{2} \quad (28)$$

and

$$\frac{H}{h} = 0.78 \left(\frac{c}{h}\right)^{2/3} \quad (29)$$

$$\frac{P_m}{M_0} = 35.34 \left(\frac{c}{h}\right)^{1/3} + 1.35 \left(\frac{c}{h}\right)^{2/3} + \frac{\pi}{4} \quad (30)$$

and

$$\frac{H}{h} = 0.86 \left(\frac{c}{h}\right)^{2/3} \quad (31)$$

$$\frac{P_m}{M_0} = 8\pi \left(\frac{c}{h}\right)^{1/2} + 2\pi \quad (32)$$

and

$$\frac{H}{h} = \left(\frac{c}{h}\right)^{1/2} \quad (33)$$

for asymmetric mixed collapse mode A, asymmetric mixed collapse mode B, extensional mode, respectively.

Examining effective crushing distance and material strain rate sensitivity, the mean dynamic crushing loads are

$$\frac{\bar{P}_m^d}{M_0} = \left[1 + \left(\frac{0.44V}{cD}\right)^{1/p} \right] \left[42.92 \left(\frac{c}{h}\right)^{1/3} + 3.17 \left(\frac{c}{h}\right)^{2/3} + 2.04 \right] \quad (34)$$

$$\frac{\bar{P}_m^d}{M_0} = \left[1 + \left(\frac{0.39V}{cD}\right)^{1/p} \right] \left[45.90 \left(\frac{c}{h}\right)^{1/3} + 1.75 \left(\frac{c}{h}\right)^{2/3} + 1.02 \right] \quad (35)$$

$$\frac{\bar{P}_m^d}{M_0} = \left[1 + \left(\frac{0.25V}{cD} \right)^{1/p} \right] \left[32.64 \left(\frac{c}{h} \right)^{1/2} + 8.16 \right] \quad (36)$$

for asymmetric mixed collapse mode A, asymmetric mixed collapse mode B, extensional mode, respectively and where $D = 6844 \text{ s}^{-1}$ and $p = 3.91$.

2. Numerical simulation

In this section, all simulation models result in axisymmetric (concertina mode) crushing for circular tubes and symmetric collapse mode for square tubes due to the prevalence and highly practical application of them. LS-DYNA is used for simulation.

2.1. Model geometry

2.1.1. Circular tube

Considering three types of circular tube with geometrical parameters shown in Table 1. The geometry comprises diameter D , wall thickness h and length L as shown in Fig. 9.

Table 1. Geometrical parameters of circular tubes, mass and initial velocity of impactor

Tube	D (mm)	h (mm)	L (mm)	M (kg)	V (m/s)
1	60	1.3	150	80	8
2	40	1	150	50	8
3	30	0.7	150	30	8

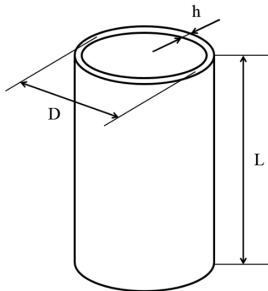


Figure 9. Geometry of a cylindrical tube.

2.1.2. Square tube

Considering three types of square tube with geometry parameters shown in Table 2. The geometry comprises length of side of square cross-section c , wall thickness h and length L shown in Fig. 10.

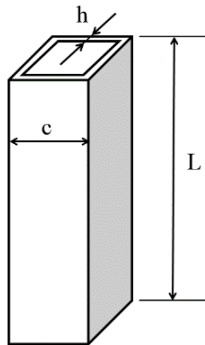


Figure 10. Geometry of a square tube.

Table 2. Geometrical parameters of square tubes, mass and initial velocity of impactor

Tube	c (mm)	h (mm)	L (mm)	M (kg)	V (m/s)
4	30	1	240	50	8
5	30	0.75	300	35	8
6	30	0.9	300	40	8

2.2. Mesh size

To depict the thin wall of tubes, Belytschko-Tsay shell element and Fully integrated shell with thickness stretch shell element are used, for comparison purposes.

The size of shell elements is approximately $2 \times 2 \text{ mm}$. This size is suitable for modelling the axial crushing of cylindrical tubes as it not only gives relatively precise results but also saves significant computing time.

The impactor is modeled as rigid body by a default eight-node solid element.

2.3. Boundary Condition and Interface Contact Condition

Clamped boundary condition is applied at the bottom of the tube, another free end tube is struck by impactor with initial velocity to be 8 m/s .

Two different contact algorithms are used. The contact between impactor and tube; another contact was applied to the column walls to avoid interpenetration of folds generated during axial collapse. These contact types utilize a penalty formulation in case a penetration is found, a proportional force to the penetration depth is applied to resist, and ultimately eliminate the penetration.

2.4. Constitutive modeling of material

The material used for thin walls is Piecewise linear plasticity with Von Mises's isotropic plasticity algorithm. This material model also included the transverse shear stress.

The tubes are made of mild steel RSt37 [11] with mechanical properties: density $\rho = 7830 \text{ kg/m}^3$, Young's modulus $E = 200 \text{ GPa}$, initial yield stress $\sigma_0 = 251 \text{ MPa}$, ultimate stress $\sigma_u = 339 \text{ MPa}$, Poisson's ratio $\nu = 0.3$, the power law exponent $n = 0.12$, coefficients of Cowper and Symonds's constitutive equation $D = 6844 \text{ s}^{-1}$ and $q = 3.91$.

3. Results and discussions

The mean crushing load P_{mean} is determined as following

$$P_{mean} = \frac{1}{\delta} \int_0^{\delta} P(\delta) d\delta \quad (37)$$

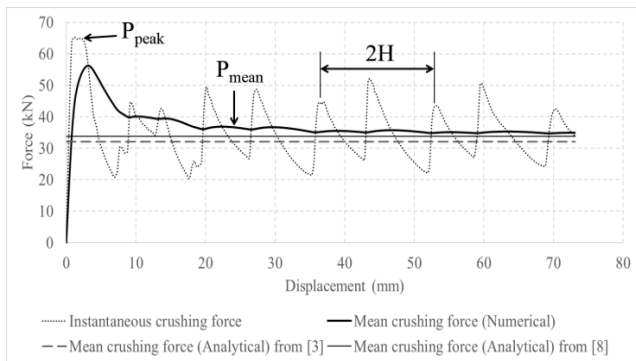
where $P(\delta)$ is an instantaneous crushing load, δ is the current crushing distance.

The mean crushing load is an indicator of energy absorbing capability of a structure when compared to the axial displacement required to absorb the energy. For thin-walled tubes, the load generally fluctuates throughout the crushing process and the highest initial load point is defined as the initial peak load, P_{peak} (shown in Fig. 11a). The maximum

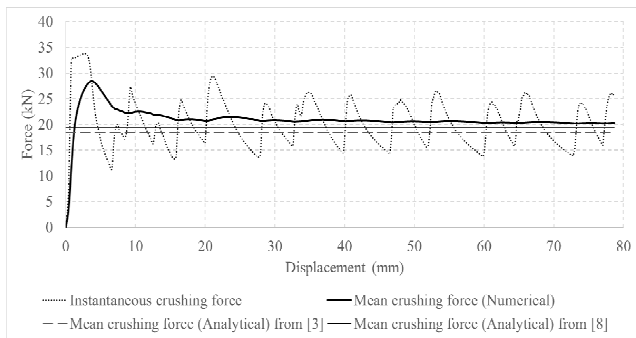
peak load is an indication of the load required to initiate collapse and begin the energy absorption process. For practical implications, the mean crushing and initial peak load are the predominant parameters in evaluating the energy absorption performance of energy absorbers.

3.1. Circular tube

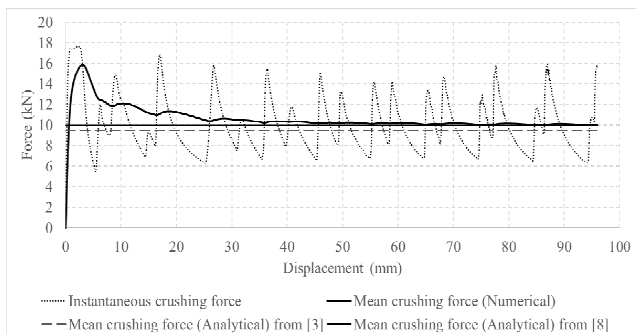
Fig. 11 is the result from numerical simulation with the data from Table 1. The dot line is obtained from numerical simulation whereas the thick solid line is calculated by (37). Additionally, two theoretical predictions are computed from [3] and [8] corresponding to (9) and (14) that are plotted by the dashed line for the former and the thin solid line for the latter.



a) Tube 1



b) Tube 2



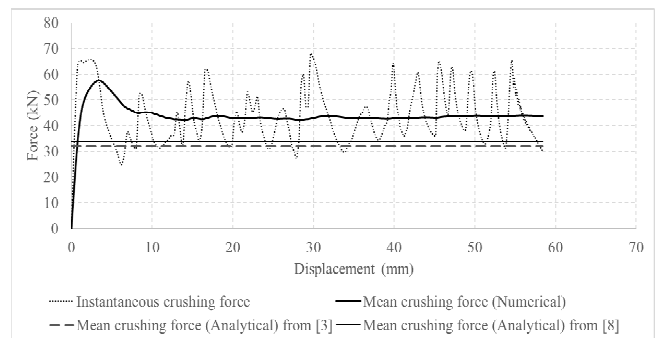
c) Tube 3

Figure 11. Crushing force response of circular tubes simulated by Belytschko-Tsay shell element.

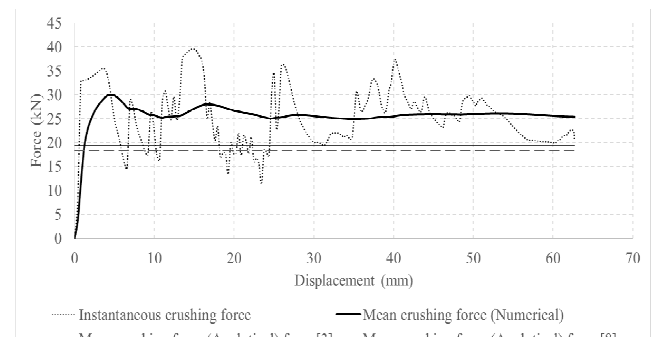
According to [2], [3], [8], the force-displacement relationship in Fig. 12 is unacceptable, not the actual

relationship obtained from experiments. For this reason, using Fully integrated shell with thickness stretch to simulate circular tubes is inaccurate, contrasted to realistic results. Instead of this, it is highly recommended to employ Belytschko-Tsay shell element for simulation of thin wall since the discrepancy between numerical simulation and theoretical results is insignificant as calculated in Table 3 and Table 4. Furthermore, it can be inferred that the theoretical formula in [8] gives a good agreement with numerical results in comparison with [3].

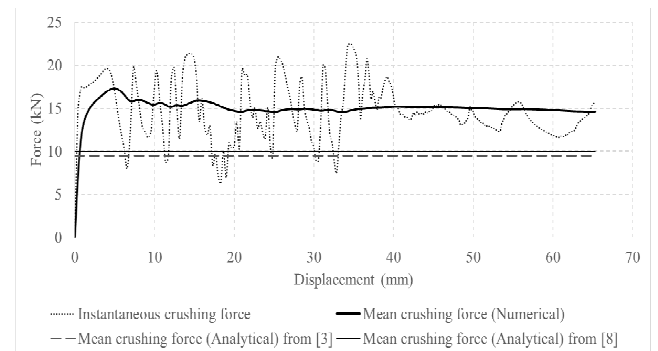
Similarly, the length of a folding element computed by [8] provides reasonable accuracy. The errors of both mean crushing force and length of a folding element is small (lower than 10%) when comparing numerical simulation to results from [8] whereas these differences are higher between current research and predictions from [3], particularly $2H$.



a) Tube 1



b) Tube 2



c) Tube 3

Figure 12. Crushing force response of circular tubes simulated by Fully integrated shell with thickness stretch.

Table 3. Comparison of mean crushing force (Belytschko-Tsay shell element)

Tube	Numerical simulation (kN)	Prediction from [3]		Prediction from [8]	
		P_m (kN)	Error (%)	P_m (kN)	Error (%)
1	34.93	32.04	9.04	33.79	3.39
2	20.28	18.38	10.32	19.39	4.58
3	9.98	9.45	5.67	9.96	0.18

Table 4. Comparison of length of a folding element (Belytschko-Tsay shell element)

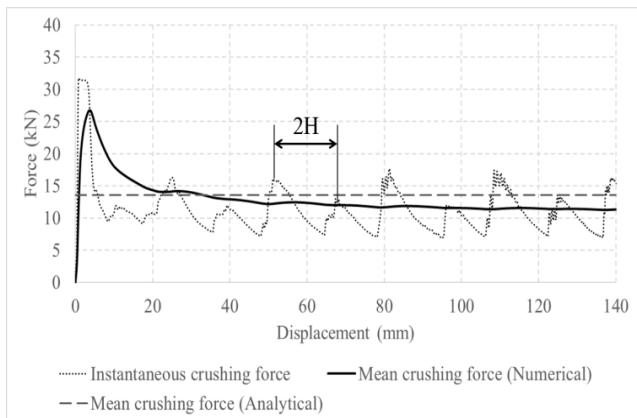
Tube	Numerical simulation (mm)	Prediction from [3]		Prediction from [8]	
		2H (mm)	Error (%)	2H (mm)	Error (%)
1	16.98	15.54	9.26	16.25	4.51
2	12.54	11.13	12.62	11.64	7.72
3	9.22	8.07	14.30	8.43	9.33

3.2. Square tube

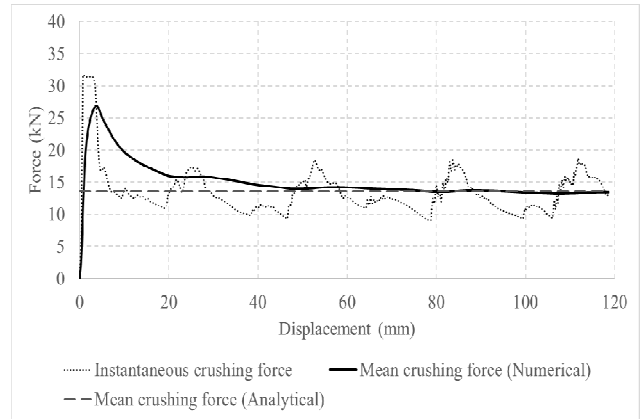
Similar to circular tubes, data in Table 2 is utilized to investigate the mean crushing force and length of a basic folding element of square tubes. The legends of Fig. 13, Fig. 14 and Fig. 15 resemble to that of circular tubes. However, the dashed line (mean crushing force from theoretical analysis) is computed by (25). The length of a basic folding element is identified by the distance between two consecutive peak loads as in Fig. 13a.

In terms of mean crushing force of square tubes, numerical simulation using Fully integrated shell with thickness stretch shell element gives a very good agreement with theoretical analysis (errors are lower than 10%) whereas square tubes employed Belytschko-Tsay shell element have larger differences (errors are approximately 20%) as presented in Table 5. Consequently, it is high suggestion for using Fully integrated shell with thickness stretch in simulation of square tubes to get appropriate and accurate outcomes.

Nevertheless, unfortunately, the disagreement of length of a basic folding element is relative high (above 10%) between numerical and theoretical analysis as can be seen in Table 6. This is also a big restriction of this paper when just solving the problem in mean crushing force existing in [6], [8].

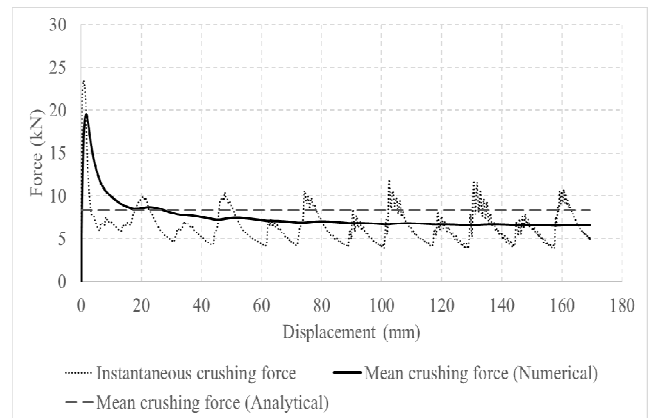


a) Belytschko-Tsay shell element

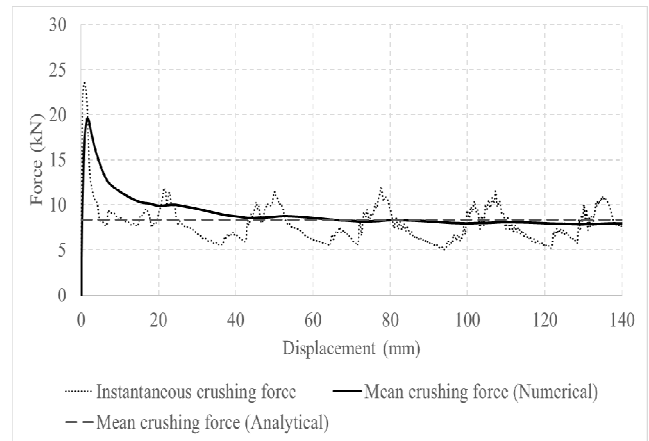


b) Fully integrated shell with thickness stretch

Figure 13. Crushing force response of square tube No. 4 simulated by different shell elements.

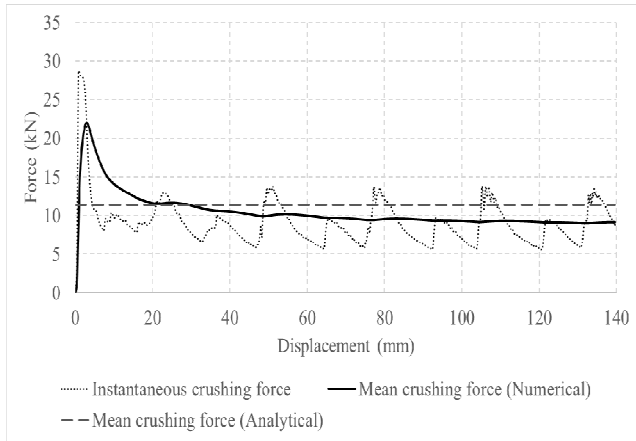


a) Belytschko-Tsay shell element

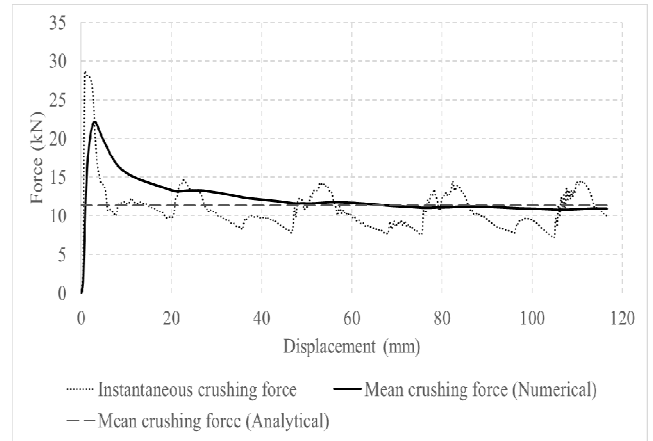


b) Fully integrated shell with thickness stretch

Figure 14. Crushing force response of square tube No. 5 simulated by different shell elements.



a) Belytschko-Tsay shell element



b) Fully integrated shell with thickness stretch

Figure 15. Crushing force response of square tube No. 6 simulated by different shell elements.

Table 5. Comparison of mean crushing force

Tube	Theoretical analysis (kN)	Numerical simulation			
		Belytschko-Tsay shell element (kN)	Error (%)	Fully integrated shell with thickness stretch (kN)	Error (%)
4	13.53	11.35	16.11	13.46	0.49
5	8.37	6.61	21.10	7.95	5.03
6	11.35	9.15	19.34	10.96	3.39

Table 6. Comparison of length of a folding element

Tube	Theoretical Analysis (mm)	Numerical simulation			
		Belytschko-Tsay shell element (mm)	Error (%)	Fully integrated shell with thickness stretch (mm)	Error (%)
4	19.12	15.32	19.89	15.63	14.93
5	17.37	14.53	16.32	14.98	13.78
6	18.46	15.24	17.44	16.25	11.98

4. Conclusions

It is reasonable and suitable to exploit Belytschko-Tsay shell element to simulate circular tubes rather than Fully integrated shell with thickness stretch based on the realistic results explained in Section 3.1. In addition, for theoretical analyses of circular tubes, mean dynamic crushing force is highly recommended to calculate by (14) instead of (9) due to the good agreement with numerical simulation.

In contrast to circular tubes, square tubes are suggested to employ shell element Fully integrated shell with thickness stretch for better results.

The length of a basic folding element of circular tubes is solved fully, but it is difficult to identify the best way for square tubes.

The above comparison and guidance is highly likely to be helpful for further investigation. Besides, this study can be an important suggestion in assessing energy absorption of both circular and square tubes.

Acknowledgements

The research for this paper was financially supported by AUN/SEED-Net, JICA for CRA Program.

Nomenclature

- c length of side of a square cross-section
- h wall thickness
- R mean radius of cylindrical shell
- L initial length of a tube
- D, p Cowper-Symonds coefficients
- 2H length of a basic folding element is estimated as Fig. 11a for circular tubes and Fig. 13a for square tubes
- M mass of impactor
- V impact velocity of impactor
- M_0 $(2\sigma_0/\sqrt{3})/(h^2/4)$ for circular tubes
 $\sigma_0 h^2/4$ for square tubes
- N number of circumferential lobes
- δ_e effective crushing distance
- σ_0 yield stress
- P_m theoretical prediction for mean static crushing load
- \bar{P}_m theoretical prediction for mean static crushing load corrected for effective crushing distance
- \bar{P}_m^a theoretical prediction for mean static crushing load corrected for effective crushing distance and

material strain rate sensitivity

References

- [1] J. M. Alexander, "An approximate analysis of the collapse of thin cylindrical shells under axial loading," *The Quarterly Journal of Mechanics and Applied Mathematics*, vol. 13, no. 1, pp. 10-15, 1960.
- [2] N. Jones, *Structural Impact*, 2nd ed., USA: Cambridge University Press, 2012, pp. 377-385.
- [3] W. Abramowicz, N. Jones, "Dynamic axial crushing of circular tubes," *International Journal of Impact Engineering*, vol. 2, no. 3, pp. 263-281, 1984.
- [4] T. Wierzbicki, "Optimum design of integrated front panel against crash," Report for Ford Motor Company, Vehicle Component Dept., 15 July 1983.
- [5] W. Abramowicz, "The effective crushing distance in axially compressed thin-walled metal columns," *International Journal of Impact Engineering*, vol. 1, no. 3, pp. 309-317, 1983.
- [6] W. Abramowicz, N. Jones, "Dynamic axial crushing of square tubes," *International Journal of Impact Engineering*, vol. 2, no. 2, pp. 179-208, 1984.
- [7] J. D. Campbell, R. H. Cooper, "Yield and flow of low-carbon steel at medium strain rates," in *Proc. Conf. on the Physical Basis of Yield and Fracture*, pp. 77-87. Inst. of Physics and Physical Soc., London (1966).
- [8] W. Abramowicz, N. Jones, "Dynamic progressive buckling of circular and square tubes," *International Journal of Impact Engineering*, vol. 4, no. 4, pp. 243-270, 1986.
- [9] T. Wierzbicki, W. Abramowicz, "On the crushing mechanics of thin-walled structures," *Journal of Applied Mechanics*, vol. 50, no. 4, pp. 727-734, Dec. 1983.
- [10] W. Abramowicz, T. Wierzbicki, "Axial crushing of multicornered sheet metal columns," *Journal of Applied Mechanics*, vol. 56, no. 1, pp. 113-120, Mar. 1989.
- [11] S. P. Santosa, T. Wierzbicki, A. G. Hanssen, M. Langseth, "Experimental and numerical studies of foam-filled sections," *International Journal of Impact Engineering*, vol. 24, no. 5, pp. 509-534, May 2000.

Biography



Hung Anh LY is a Lecturer in the Department of Aerospace Engineering – Faculty of Transport Engineering at Ho Chi Minh City University of Technology (HCMUT). He received his BEng in Aerospace Engineering from HCMUT in 2005, his MEng in Aeronautics and Astronautics Engineering from Bandung Institute of Technology - Indonesia (ITB) in 2007 and his DEng in Mechanical and Control Engineering from Tokyo Institute of Technology – Japan (Tokyo Tech) in 2012. He stayed at ITB and Tokyo Tech for one month as a researcher in 2012 and 2013. He is a member of the New Car Assessment Program for Southeast Asia (ASEAN NCAP). His main

research interests include strength of structure analysis, impact energy absorbing structures and materials.



Thinh THAI-QUANG is currently a final-year student at the Department of Aerospace Engineering, Faculty of Transportation Engineering, Ho Chi Minh City University of Technology (HCMUT), Vietnam. He is going to receive the Bachelor's degree in Aerospace Engineering from HCMUT in April, 2015. His research interests include the areas of structural impact, finite element methods, and structural mechanics.